Int. J. Therm. Sci. (2001) 40, 133–144

S1290-0729(00)01202-3/FLA

Measurement of thermophysical properties of polyurethane foam insulation during transient heating

Ganesh Venkatesan [a], Guang-Pu Jin [a], Ming-Chien Chyu [a]*, Jian-Xue Zheng [a], Tse-Yao Chu [b]

[a] *Department of Mechanical Engineering, Texas Tech University, Lubbock, TX 79409-1021, USA*

[b] *Sandia National Laboratories, Albuquerque, NM 87185, USA*

(Received 21 October 1999, accepted 14 March 2000)

Abstract — Thermal conductivity and heat capacity of polyurethane foam insulation of 374 kg·m^{-3} density were measured up to 200 °C. Thermal conductivity and heat capacity were determined by transient temperature data taken across the foam specimen when one surface was subjected to a uniform heat flux input. The transient temperature data were then processed by a parameter estimation computer code to determine the effective thermal conductivity and heat capacity. Linear thermal conductivity and heat capacity variations with temperature were determined by providing the property values at two different temperatures. Analyses for sequential estimates, residuals, sensitivity coefficients were conducted for all property data obtained to assure accuracy. The results were compared with published data as well as an existing model. It was found that the existing model for thermal conductivity of foam materials tends to underpredict the experimental data. © 2001 Éditions scientifiques et médicales Elsevier SAS

inverse heat conduction analysis / thermal conductivity / heat capacity

Nomenclature

C	heat capacity $= \rho c_p$	J·m^{-3}·K^{-1}
c_p	specific heat at constant pressure	J·kg^{-1}·K^{-1}
d	cell diameter	m
e	residual	K
f_s	fraction of the polymer in the struts	
K	Rosseland mean extinction coefficient of the foam	m^{-1}
k	thermal conductivity	W·m^{-1}·K^{-1}
k_{eff}	effective thermal conductivity	W·m^{-1}·K^{-1}
q''	heat flux	W·m^{-2}
T	temperature	°C or K
t	time	s
t_e	the end of the time period that temperature data are considered	s
u	uncertainty	
U	percentage uncertainty	
x	distance from the heated surface	in

Greek symbols

δ	volume fraction of voids	
ρ	density	kg·m^{-3}
σ	Stefan–Boltzmann constant $= 5.67 \cdot 10^{-8}$	W·m^{-2}·K^{-4}

Subscripts

c	calculated
cond	conduction in solid
eff	effective
f	foam
m	measured
p	polymer
rad	radiation
s	solid

1. INTRODUCTION

Heat transfer in a polyurethane foam material takes place by conduction through the solid cell walls and struts, conduction through the gas-filled interior, and radiation through the foam. Natural convection of gas within a cell is insignificant because of very low Rayleigh number. Skochdopole [1] conducted of a simple experiment by reversing the hot and cold plates of a modified guarded hot plate unit in order to maximize and minimize convec-

* Correspondence and reprints.
E-mail address: mchyu@coe.ttu.edu (M.-C. Chyu).

tion, and showed that heat transfer by convection does not exist for cell diameters smaller than 4 mm. Most polyurethane foams have closed cells about one order of magnitude smaller than 4 mm, and therefore, heat transfer due to convection is negligible [2].

Valenzuela [3] showed that published heat transfer models underestimated foam effective thermal conductivity if the contribution due to radiation was not considered. Cunningham et al. [4] and Glicksman et al. [5] indicated that the radiation contribution could account for approximately 30 % of the measured effective conductivity at room temperature. Many existing models, including those of Skochdopole [1], Cunningham et al. [4], Glicksman et al. [5], and Schuetz et al. [6], postulated that the effective thermal conductivity of the foam is the sum of contributions of three transport paths, i.e.

$$k_{\text{eff}} = k_{\text{cond}} + k_{\text{rad}} + k_{\text{gas}} \tag{1}$$

where k_{cond} is the contribution due to conduction through solid matrix, k_{rad} is the contribution due to radiation, and k_{gas} is the contribution due to conduction through gas.

In most of the available heat transfer models, the solid and gas conduction aspect of the problem is usually approached based on an idealized matrix geometry, and an either exact or approximate, usually one-dimensional solution thereof. The radiation aspect of the problem has been treated by considering the cell walls to be either opaque or transparent.

Thermal conductivities of polyurethane foams have been measured using steady-state standard methods such as ASTM C-177, C-518 or C-1114 [7]. However, the present literature search revealed that information on the variation of thermal conductivity with temperature for different polyurethane foam densities was not available. Published data on the heat capacity of polyurethane foams are also scarce. Beck and Arnold [8] developed a procedure for determining the thermal properties from transient temperature and heat flux measurements. This method involving parameter estimation analysis has been used to determine the thermal properties of a variety of materials by several authors. Dowding et al. [9] used this technique to determine the temperature-dependent thermal properties of carbon composites.

Polyurethane as a thermal insulation and encapsulant may be subjected to high heat due to fire or other abnormal conditions. The objective of the present research is to determine the thermal conductivity and heat capacity of polyurethane foam insulation during transient heating through experiment coupled with a parameter estimation analysis, and to compare the result with published data and an existing analytical model. Polyurethane foam of 374 $\text{kg}\cdot\text{m}^{-3}$ density was tested up to 200 °C.

2. ANALYSIS

In the present experiment, a one-dimensional foam test specimen was heated with an electric heater on one surface with the other surfaces insulated. Heat conduction within the test specimen is governed by the following formulation (*figure 1*):

$$\begin{aligned}
&\frac{\partial}{\partial x}\left[k(T)\,\frac{\partial T}{\partial x}\right] = C(T)\frac{\partial T}{\partial t}, && T(x,t),\ 0<x<L,\ t>0\\
&-k\,\frac{\partial T}{\partial x} = q_0'', && x=0,\ t>0\\
&\frac{\partial T}{\partial x} = 0, && x=L,\ t>0\\
&T = T_0, && 0\le x\le L,\ t=0
\end{aligned} \tag{2}$$

In the above formulation, the thermal conductivity $k(T)$ and heat capacity $C(T)$ are unknown, while data of temperature variation with time at different locations can be measured. These temperature data are used to determine the thermal conductivity and heat capacity of the specimen through a method involving parameter estimation analysis. The functional forms that thermal conductivity (k) and heat capacity (C) vary with the space coordinate are assumed. It is expedient to assume that both k and C vary linearly and continuously across the specimen thickness (x-coordinate). The number of spatial temperature data across the specimen must equal or exceed the number of unknown parameters in the k and

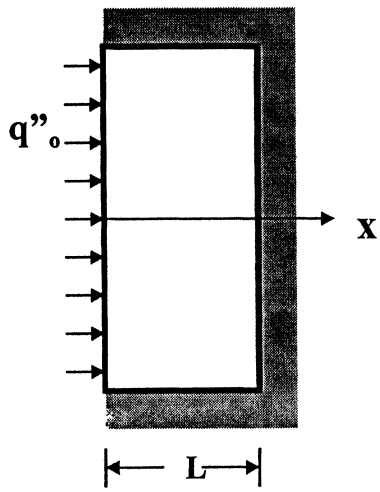

Figure 1. Heat conduction model.

C functions. Thus, the inverse heat conduction problem can be regarded as a problem of parameter estimation. Such a problem can be solved by the Levenberg–Marquardt method which solves nonlinear least-squares equations by iteration. The solution method will involve solving the direct conduction problem with finite-difference method, computing the sensitivity coefficients for each parameters, and calculating the parameters by iteration.

A parameter estimation computer code similar to that used by Dowding et al. [9], commercialized by Beck Engineering Consultants Company, Okemos, Michigan, was employed in the present study. In a two-parameter case, the code provides an estimation of k and C values assuming both are independent of T; i.e. $k = \text{const}$, and $C = \text{const}$. In a four-parameter case, the code estimates linear k and C variations with temperature by providing the k and C values at two different temperatures.

3. EXPERIMENT

In an experiment that can generate useful data for inverse heat conduction analysis, it is necessary to control the thermal boundary condition in terms of the exact amount of heat input to the test specimen. However, control of the heat loss from the backside of a heater applied to the foam specimen surface is difficult. The present experimental facility featured an electric heater sandwiched between two identical pieces of test insulation (approximately $30 \times 30 \times 15$ cm^3), as shown in *figure 2* and in more detail in *figure 3*. The two pieces of test insulation were identical in terms of composition, density, thermal properties, dimensions, thermal boundary condition, etc.; therefore, identical thermal behavior was expected. In such an arrangement, each insulation was subjected to a heat input rate equal to $1/2$ of the total heat rate generated by the heater. All the other surfaces of the test insulation were insulated in order to eliminate heat loss, if any (*figure 3*). Thermocouples were installed at strategic locations to monitor change of temperature distribution throughout the specimen during heating (*figure 4*).

A flexible silicone rubber electric heater was sandwiched between the two test specimens, and its heating power was controlled by a powerstat, with the power measured by a voltmeter and an ammeter, as shown in *figure 2*. Temperature data were taken and processed by a computer-controlled data acquisition system. Polyurethane foam of 374 kg·m^{-3} density was tested up to 200 °C.

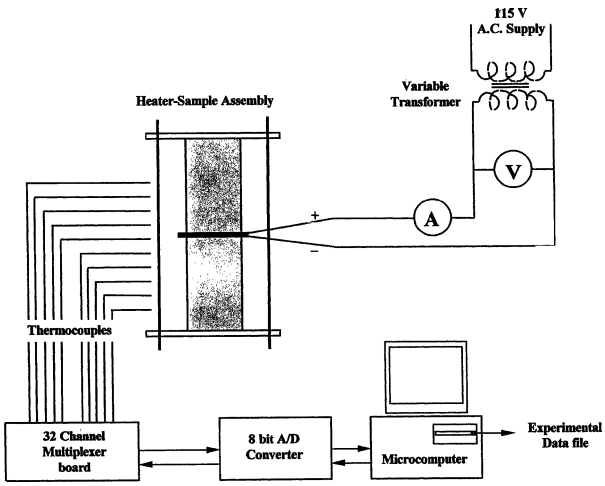

Figure 2. Experimental facility.

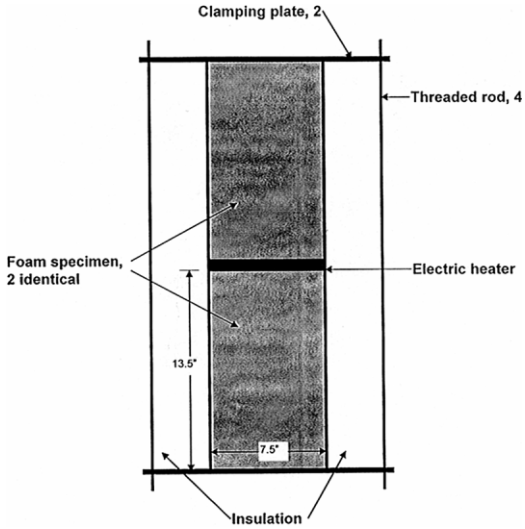

Figure 3. Test section.

The errors of the thermophysical property results obtained in this study were assessed by the method of sequential perturbations [10], where the total uncertainty of a set of data is estimated by integrating the uncertainties due to errors associated with individual participating parameters. The total uncertainty in k_{eff} was calculated as $\pm 13\,\%$, and the total uncertainty in C was $\pm 11\,\%$. Details of error analysis can be found in appendix.

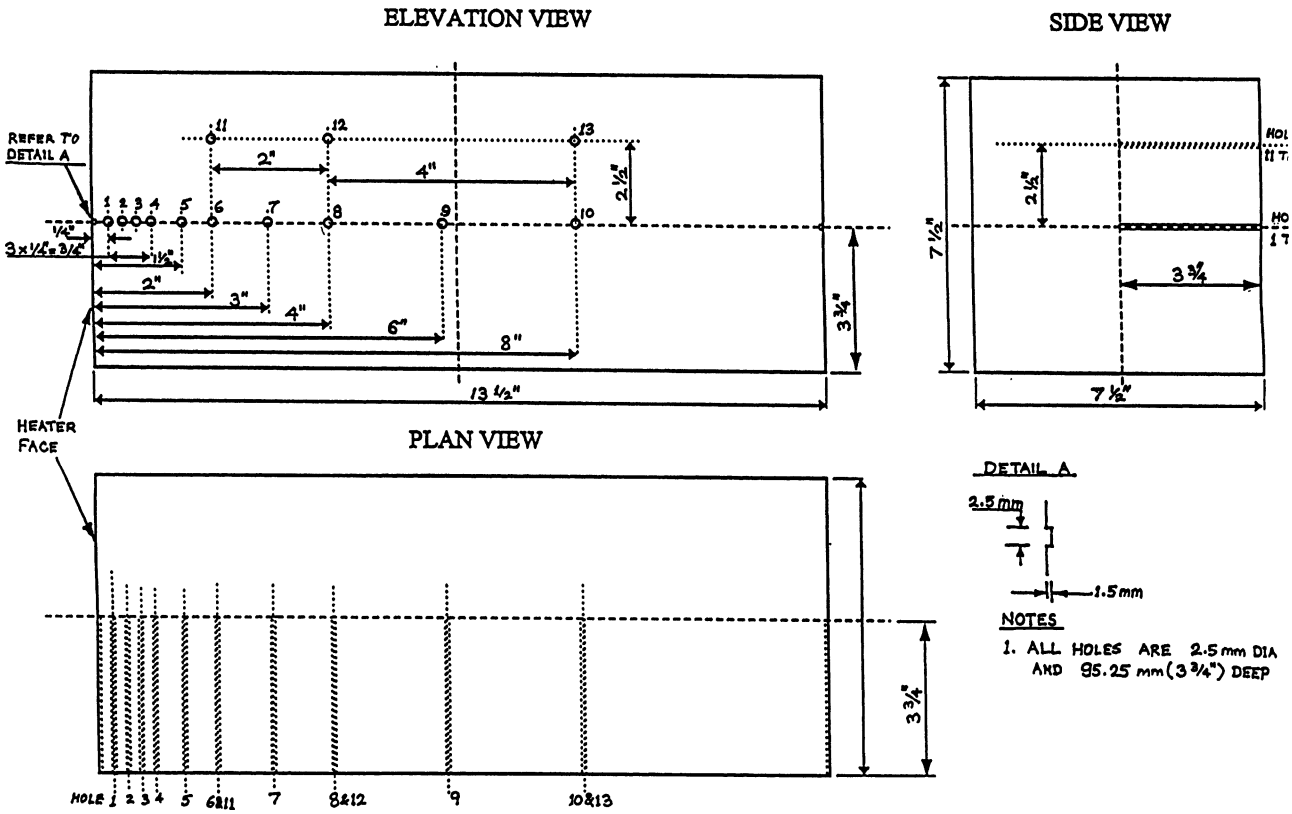

Figure 4. Dimensions of foam specimen.

4. RESULTS AND DISCUSSION

4.1. General

Three tests were conducted with the 374 kg·m^{-3} density specimen: 30 to 80 °C, 30 to 120 °C, and 30 to 200 °C. During the experiment, the thermocouples positioned 2.5 in offset from the centerline, and 2 in from the heated surface, showed a maximum deviation of 0.2 K compared to the centerline temperature recorded at the same longitudinal location. This indicated that temperature gradient in the lateral direction, and, therefore, the side heat loss, was negligible, and heat conduction virtually took place only in the longitudinal direction. All the thermocouple readings at corresponding locations in two individual specimens tested simultaneously were compared to ensure symmetry. The deviations were always less than 0.5 K in all tests.

It was observed that when the heater temperature was above 150 °C, the surface of the specimen in contact with the heater started to turn brown and to bulge sideways (parallel to the heated surface), while the central region of the heated surface caved in. Fumes were generated and cracks were developed in the corners of the specimens in contact with the heaters.

4.2. 80 °C test results

4.2.1. Results without heater and contact resistance effect

It was found in the present study that if only the test specimen was considered in the parameter estimation analysis, thermophysical properties could not be estimated accurately. *Figure 5* exhibits a typical result that the estimated effective thermal conductivity (k_{eff}) values at both 30 °C and 80 °C vary with the test time t_{e} within which temperature data were used for k_{eff} estimation. It is shown that if the test specimen only, without the heater, was considered in the analysis, estimated k_{eff} does not reach a steady value. Therefore, no conclusion regarding the $k_{\text{eff}}(T)$ function can be reached. An accurate estimate

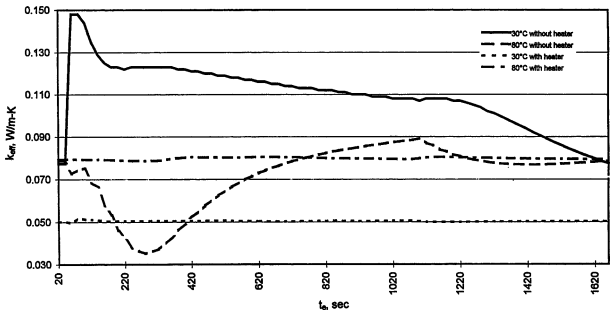

Figure 5. Comparison of sequential estimates of thermal conductivity obtained by models with and without heater effect.

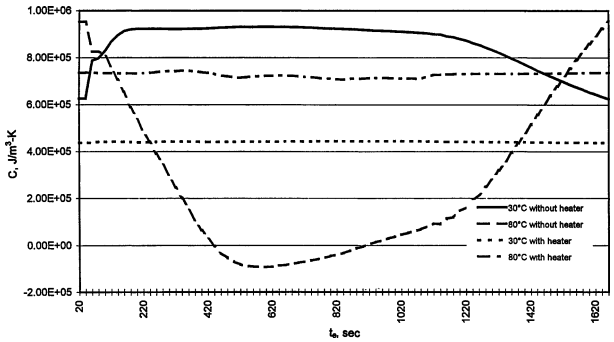

Figure 6. Comparison of sequential estimates of volumetric heat capacity obtained by models with and without heater effect.

of the property should be independent of t_e. A similar behavior is demonstrated in *figure 6* by the C values at both 30 °C and 80 °C estimated without considering the heater effect. The problem was solved by taking into account in the analysis the thermal effect of the heater and the contact resistance between the heater and the test specimen, as recommended by Dowding et al. [9]. Apparently, the contact resistance plays an important role by affecting the temperature distribution in the specimen.

4.2.2. Short duration tests for heater and contact resistance

In order to take the heater and the contact resistance into account, the heater along with the test specimen needs to be included in the model, making it a two-region heat conduction problem for each of the two specimens. In a similar experiment estimating the thermal properties of a carbon–carbon composite, Dowding et al. [9] experimentally estimated the effective thermal conductivity of the electric heater, including the contact resistance effect, by conducting a series of short duration experiments. A short duration test has to be reconducted every time after the test setup is reconfigured because reconfiguration of the setup changes the contact resistance.

In the present experiment, similar short tests as that carried out by Dowding et al. [9] were conducted to determine the heater's effective thermal conductivity including the contact resistance effect. In a typical short test, heat flux generated by the electric heater was approximately 370 $W \cdot m^{-2}$, with test duration of about 30 s. The test duration was so short that by the end of the test, only the first thermocouple (on the specimen's heated surface) recorded a significant temperature rise, while all the other thermocouple readings were virtually maintained at the initial (surrounding) temperature. Although the effective thermal conductivity of the heater was determined based on estimated properties of the test specimen and assumed volumetric heat capacity of the heater, the final results of estimated specimen properties were found not significantly affected by the accuracy of those estimated and assumed values, as also reported by Dowding et al. [9].

4.2.3. Model with heater and contact resistance effect

The thermophysical properties of polyurethane foam were determined by including the heater and contact resistance effect in the model, again using the same parameter estimation code. Both two-parameter and four-parameter cases were studied for the 374 $kg \cdot m^{-3}$ specimen. The results based on a set of temperature test data with the maximum specimen temperature at about 80 °C are shown in *tables I* and *II*. Since the two specimens on both sides of the heater were identically instrumented, two different estimates of properties plus another estimate based on the average temperature data were obtained. For all the k_{eff} and C data presented in this work, the contact resistance was reevaluated by means of the aforementioned short-duration test each time after the test specimen was reinstalled and the contact resistance between the heater and the specimen was changed.

4.2.4. Sequential estimate

The results exhibited in *tables I* and *II* are based on sequential estimates of properties, such as that shown in *figures 5* and *6* (30 °C and 80 °C with heater). The sequential estimates demonstrate how the estimated properties vary as additional temperature data are considered. With the heater and contact-resistance effect taken into account, both k_{eff} and C approach to steady values as t_e increases. Relatively large variation is observed only at the beginning of the test (small t_e), because there is not enough information to determine the property. A correct

TABLE I
Estimated thermal conductivity and heat capacity from 30 to 80 °C, 374 kg·m^{-3} specimen. Two-parameter case ($k_{\text{eff}} = \text{const}$, $C = \text{const}$).

	k_{eff} W·m^{-1}·K^{-1}	C J·m^{-3}·K^{-1}	Locations (x) of thermocouple readings used in analysis, in
Specimen A	0.0682 ± 0.0034	$5.13{\cdot}10^5 \pm 1.25{\cdot}10^4$	0, 0.25, 0.5, 0.75, 1.0
Specimen B	0.0647 ± 0.0021	$4.88{\cdot}10^5 \pm 9.27{\cdot}10^3$	0, 0.25, 0.5, 0.75, 1.0
Average	0.0664 ± 0.0027	$5.00{\cdot}10^5 \pm 1.08{\cdot}10^4$	0, 0.25, 0.5, 0.75, 1.0

TABLE II
Estimated thermal conductivity and heat capacity from 30 to 80 °C, 374 kg·m^{-3} specimen. Four-parameter case (linear $k_{\text{eff}}(T)$ and $C(T)$).

	k_{eff} W·m^{-1}·K^{-1}			C J·m^{-3}·K^{-1}			Locations (x) of thermocouple readings used in analysis, in
	30 °C	80 °C	Fitted $k_{\text{eff}}(T)$, T: °C	30 °C	80 °C	Fitted $C(T)$, T: °C	
Specimen A	0.0503 ±0.0017	0.0794 ±0.0013	$0.0328 + 0.000582T$	$4.37{\cdot}10^5$ ±$1.03{\cdot}10^4$	$7.36{\cdot}10^5$ ±$3.69{\cdot}10^4$	$2.58{\cdot}10^5 + 5.98{\cdot}10^3T$	0, 0.25, 0.5, 0.75, 1.0
Specimen B	0.0512 ±0.0025	0.0713 ±0.0018	$0.0392 + 0.000401T$	$4.27{\cdot}10^5$ ±$1.69{\cdot}10^4$	$6.36{\cdot}10^5$ ±$5.84{\cdot}10^4$	$3.02{\cdot}10^5 + 4.17{\cdot}10^3T$	0, 0.25, 0.5, 0.75, 1.0
Average	0.0508 ±0.0015	0.0751 ±0.0011	$0.0363 + 0.000485T$	$4.32{\cdot}10^5$ ±$1.07{\cdot}10^4$	$6.83{\cdot}10^5$ ±$3.81{\cdot}10^4$	$2.82{\cdot}10^5 + 5.02{\cdot}10^3T$	0, 0.25, 0.5, 0.75, 1.0

estimation of the property must be independent of time period t_e. The results in *tables I* and *II* as well as all the k_{eff} and C data for different foam densities and temperatures presented in this work are t_e independent.

4.2.5. Residuals

A quantity that can be observed to demonstrate the accuracy of the estimated property is residual. Residual e_{ij} is the difference between the measured temperature $T_{\text{m},ij}$ and the calculated temperature $T_{\text{c},ij}$ for a particular time (t_i) and thermocouple location (x_j), calculated as

$$e_{ij} = T_{\text{m},ij} - T_{\text{c},ij} \tag{3}$$

Figure 7 presents the residual data for a 374 kg·m^{-3} specimen. Of all the five sensors used in the analysis, the one at the heated surface ($x = 0$) has the maximum residual. However, the magnitude of the residual is approximately within only ±0.2 °C, except immediately after the heater was turned on ($t = 0$ s) and turned off ($t = 1086$ s). Even the maximum residual during the test, observed immediately after the heater was turned off, is only about 1.7 % of the temperature rise during the experiment. The residual at other locations, such as $x = 1.0$ in shown in *figure 7*, is within approximately ±0.2 °C. The small residuals indicate small errors in the result of the inverse conduction analysis.

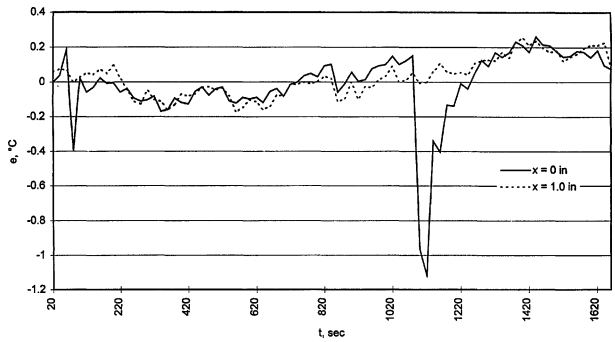

Figure 7. Temperature residuals.

4.2.6. Sensitivity coefficients

Sensitivity coefficient is the first derivative of temperature with respect to the estimated property. It indicates how well the experiment is designed [9]. In general, the sensitivity coefficients are desired to be large and uncorrelated (linearly independent). *Figure 8* shows the sensitivity coefficients of k_{eff} and C for a specimen at 30 °C for two sensor locations (0 and 1.0 in). It is observed that the sensitivity coefficients for both sensors are correlated only for a very short time period during initial heating, and uncorrelated for the rest of test period. The above analyses for sequential estimates, residuals, and sensitiv-

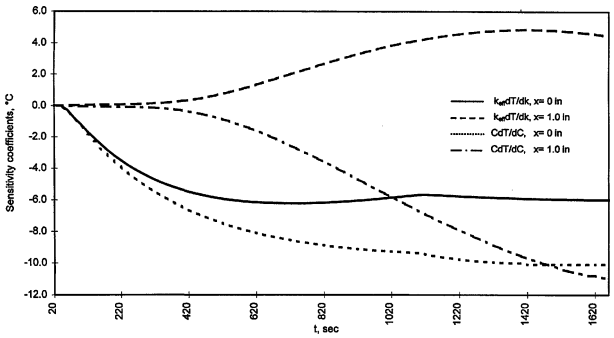

Figure 8. Sensitivity coefficients for estimated properties at 30 °C.

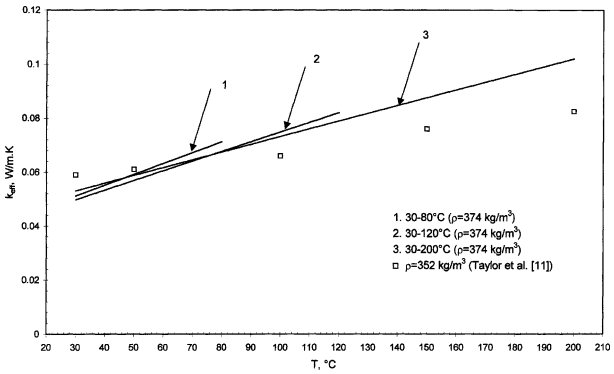

Figure 9. Estimated effective thermal conductivity.

ity coefficients were conducted for all the thermophysical property data presented in this work.

4.3. 120 °C test results

Tests were also conducted for the maximum specimen temperature (at the heated boundary surface) reaching 120 °C. The linear $k_{\text{eff}}(T)$ and $C(T)$ functions obtained based on average data are plotted in *figures 9* and *10*, along with those of the 30–80 °C test for comparison. It is shown that for both $k_{\text{eff}}(T)$ and $C(T)$, the results for two different temperature ranges well agree. In *figure 9*, the fact that the 30–120 °C function has a smaller slope than the 30–80 °C function seems to suggest a negative $\mathrm{d}^2k_{\text{eff}}/\mathrm{d}T^2$. A similar trend is also observed with C in *figure 10*. The sequential estimates of k_{eff} and C for the 120 °C test with the 374 kg·m^{-3} specimen are exhibited in *figure 11*, showing the data are eventually independent of t_{e}. Numerical data as well as fitted functions of the 120 °C test are included in the summary table for the 374 kg·m^{-3} specimen, *table III*.

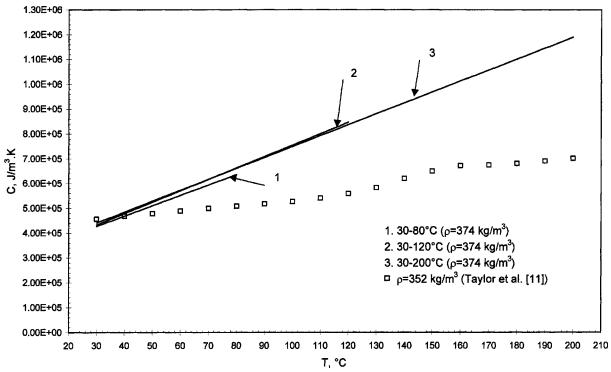

Figure 10. Estimated heat capacity.

4.4. 200 °C test results

The results of the 30–200 °C test with the 374 kg·m^{-3} specimen are included in *figures 9* and *10* for k_{eff} and C, respectively. Estimated k_{eff} and C data as well as fitted functions are also included in *table III*. The sequential estimates of k_{eff} and C values are exhibited in *figure 12*, showing that the estimated values are independent of time period.

In both *figures 9* and *10*, the three lines for different temperature ranges with the 374 kg·m^{-3} specimen demonstrate satisfactory repeatability. The experimental results demonstrate that both k_{eff} and C increase with T, and $k_{\text{eff}}(T)$ and $C(T)$ functions are close to linear in the present temperature range of 30 to 200 °C. In *figure 9*, the three lines indicate a slight decrease in $\mathrm{d}k_{\text{eff}}/\mathrm{d}T$ with temperature, i.e. a negative $\mathrm{d}^2k_{\text{eff}}/\mathrm{d}T^2$.

Also included in *figures 9* and *10* are the data of a 352 kg·m^{-3} density foam sample from Taylor et al. [11]. Both their k and C data are lower than the present data. Possible reasons for the discrepancy are as follows:

(a) The density of their specimen is 11 % lower than the present specimen; however, it is closest to our specimen we could find. The solid phase in a polyurethane foam usually consists of the organic substance along with other ingredients added for a variety of reasons, such as foaming agents, fire retardants and dyes or pigments. The physical properties of the resultant foam can vary greatly depending on the specific types and amounts of ingredients added as well as the foaming procedure followed.

(b) In their work, the thermal conductivity was not measured; instead, it was calculated based on measured thermal diffusivity, specific heat, and density.

(c) The thermal diffusivity was measured using the laser flash technique where the front face of a small disc-shaped sample was subjected to a short laser burst and

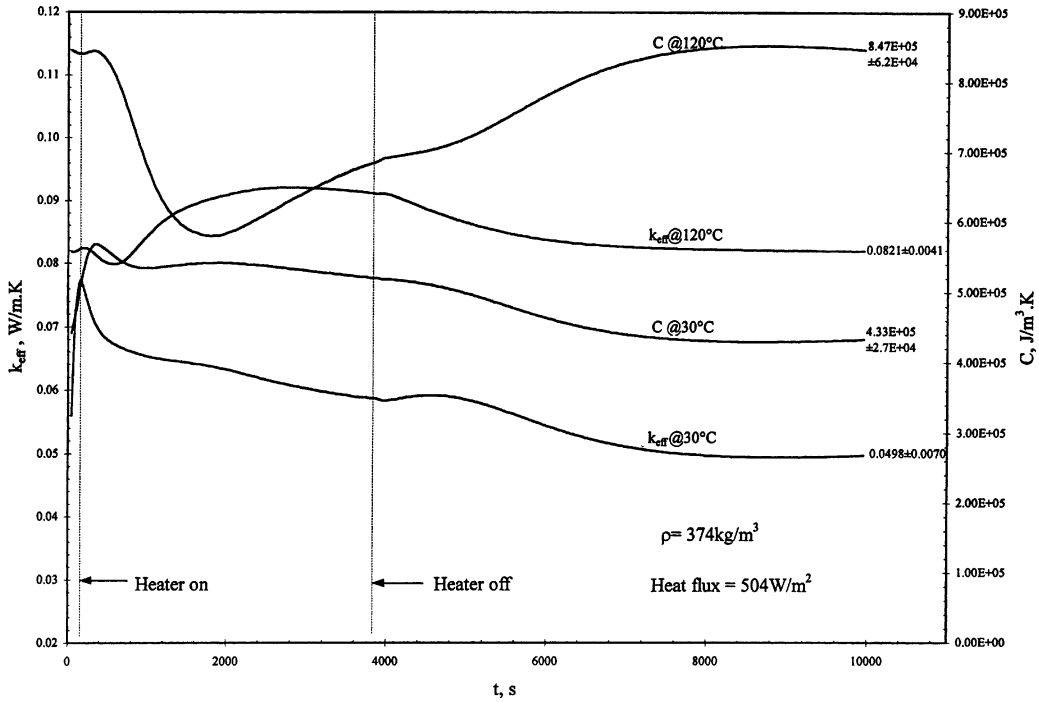

Figure 11. Sequential estimates of effective thermal conductivity and heat capacity for 120 °C test with 374 kg·m^{-3} specimen.

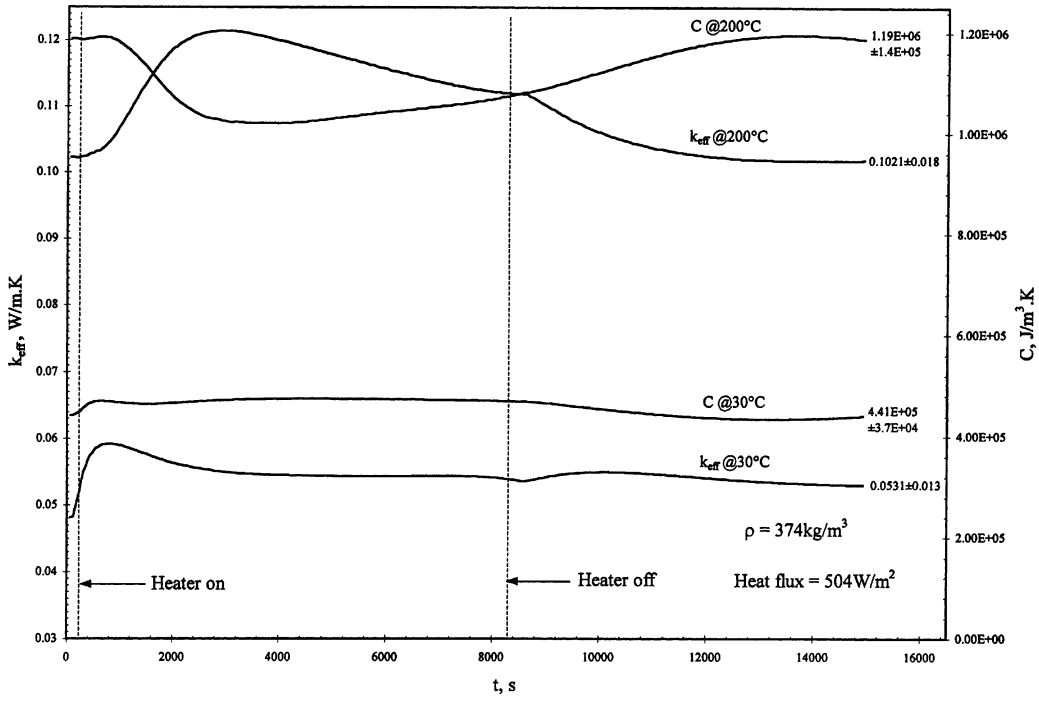

Figure 12. Sequential estimates of effective thermal conductivity and heat capacity for 200 °C test with 374 kg·m^{-3} specimen.

TABLE III
Estimated thermal conductivity and heat capacity for 374 kg·m^{-3} specimen.

		k_{eff}, W·m^{-1}·K^{-1}	C, J·m^{-3}·K^{-1}
Test 1, 30 to 80 °C	30 °C	0.0508 ± 0.0015	$4.32{\cdot}10^5 \pm 1.1{\cdot}10^4$
	80 °C	0.0751 ± 0.0011	$6.83{\cdot}10^5 \pm 3.8{\cdot}10^4$
	Fitted function, T: °C	$k_{\text{eff}}(T) = 0.0363 + 0.000485T$	$C(T) = 2.82{\cdot}10^5 + 5.02{\cdot}10^3 T$
Test 2, 30 to 120 °C	30 °C	0.0498 ± 0.0070	$4.33{\cdot}10^5 \pm 2.7{\cdot}10^4$
	120 °C	0.0821 ± 0.0041	$8.47{\cdot}10^5 \pm 6.2{\cdot}10^4$
	Fitted function, T: °C	$k_{\text{eff}}(T) = 0.0392 + 0.000402T$	$C(T) = 2.95{\cdot}10^5 + 4.60{\cdot}10^3 T$
Test 3, 30 to 200 °C	30 °C	0.0531 ± 0.0130	$4.41{\cdot}10^5 \pm 3.7{\cdot}10^4$
	200 °C	0.1021 ± 0.018	$1.19{\cdot}10^6 \pm 1.4{\cdot}10^5$
	Fitted function, T: °C	$k_{\text{eff}}(T) = 0.0444 + 0.000288T$	$C(T) = 3.08{\cdot}10^5 + 4.41{\cdot}10^3 T$

the resulting rear face temperature rise was analyzed. Depending on the laser heat flux and the sample thermal diffusivity, a great temperature gradient across the sample disc could be generated and causing a significant error in the thermal diffusivity measurement if only the rear face temperature was analyzed assuming constant thermophysical properties across the disc.

(d) The specific heat, based on which the thermal conductivity was calculated, was measured after the sample had been heated to 260 °C in a previous mass loss experiment. The sample was reported to have experienced a 2.43 % mass loss and to have "turned brown" at this temperature. Such changes were most likely irreversible and might have permanently changed the thermophysical properties of the foam sample.

4.5. Comparison with existing model

The present results were compared with the existing analytical model for heat transfer through a cellular foam insulation by Glicksman et al. [5]. The model considers the effective thermal conductivity of a foam insulation as the superposition of contributions due to (a) heat conduction through the solid polymer, (b) heat conduction through the gas in the cell, and (c) thermal radiation, as substantiated by the following equation:

$$k_{\text{eff}} = k_{\text{cond}} + k_{\text{rad}} + k_{\text{gas}} \tag{4}$$

The contribution due to conduction through the solid polymer, k_{cond}, can be expressed as

$$k_{\text{cond}} = \frac{2}{3} k_{\text{p}} \left(1 - \frac{f_{\text{s}}}{2}\right)(1 - \delta) \tag{5}$$

where k_{p} is the thermal conductivity of solid polymer. The value of thermal conductivity of polyurethane is generally taken as 0.250 W·m^{-1}·K^{-1}, while values of a wide range of variability, from 0.167 to 0.348 W·m^{-1}·K^{-1}, have been quoted in the literature [12]. The parameter f_{s} is the fraction of the polymer in the struts. A strut is the material formed at the intersection of three cell walls. A value of 0.8 was used for f_{s} by Collishaw and Evans [12]. $(1 - \delta)$ is the volume fraction of the foam occupied by the solid, and can be calculated as

$$1 - \delta = \frac{\rho_{\text{f}}}{\rho_{\text{s}}} \tag{6}$$

where ρ_{s} is the density of solid polyurethane, and is 1 251 kg·m^{-3} for the present specimen, and 1 150 kg·m^{-3} was used by Dostal [13]. The term for conduction through the gas in the cell is calculated by the following correlation for thermal conductivity of CO_2, the blowing agent of the tested foam specimens, based on the thermal conductivity data in Incropera and DeWitt [14, table A.4]:

$$k_{\text{gas}} = 0.001(0.0793T - 6.99) \tag{7}$$

where T is in K and k_{gas} in W·m^{-1}·K^{-1}. The radiation term in the effective thermal conductivity equation is calculated by

$$k_{\text{rad}} = 16 \frac{\sigma T^3}{3K} \tag{8}$$

where T is again in K and K is the Rosseland mean extinction coefficient of the foam, and is given as

$$K = 4.10 \frac{\sqrt{f_{\text{s}} \rho_{\text{f}} / \rho_{\text{s}}}}{d} \tag{9}$$

where d is the cell diameter. Values of the parameters used in the present calculation are summarized in *table IV*.

TABLE IV
Summary of parameters used in model calculation.

Parameter	Value	Reference
d	$3.9{\cdot}10^{-4}$ m	Chu, 1997; Newbury, 1997
ρ_f	374 kg·m^{-3}	measured
ρ_s	1 251 kg·m^{-3}	Chu, 1997
k_p	0.25 W·m^{-1}·K^{-1}	[12]
f_s	0.8	[12]
k_{gas}	$0.001(0.0793T - 6.99)$ W·m^{-1}·K^{-1}, T: K	[14], fitted curve

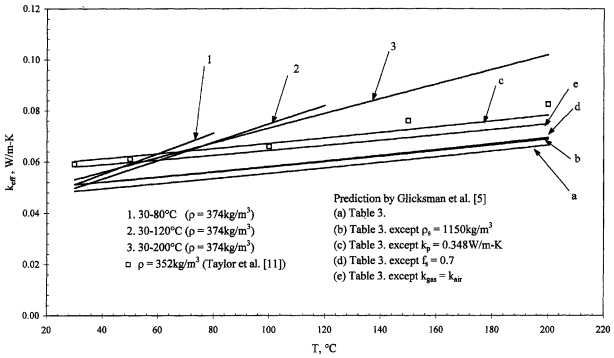

Figure 13. Comparison of experimental k_{eff} data with the model.

The result of calculated effective thermal conductivity for polyurethane foam using the above model by Glicksman et al. [5] as well as parameters listed in *table IV*, is compared with the present experimental result in *figure 13*. Also included are the experimental data for a 352 kg·m^{-3} polyurethane foam by Taylor et al. [11]. The predicted result (curve (a)) is significantly lower than both the present and Taylor et al. [11] experimental data.

Since variations are possible with some parameters used in the model, several additional cases were calculated in order to demonstrate a possible variation range of the predicted k_{eff} using the model by Glicksman et al. [5]. Plotted in *figure 13*, the predicted results include curve (b) based on all the parameters in *table IV* except $\rho_s = 1\,150$ kg·m^{-3}, a value given by Dostal [13], curve (c) based on all the parameters in *table IV* except $k_p = 0.348$ W·m^{-1}·K^{-1}, a value quoted by Collishaw and Evans [12], curve (d) based on all the parameters in *table IV* except $f_s = 0.7$, just to demonstrate the sensitivity of the result to a variation of f_s, and curve (e) based on all the parameters in *table IV* except CO_2 was replaced with air as the gas in the cells and $k_{gas} = 0.001(0.072T + 4.7)$ W·m^{-1}·K^{-1} for air. Curve (e) was of interest based on the consideration of possible aging of the foam specimen. Aging is a phenomenon that the composition of a gas in the cells of a polymeric foam does not remain constant with time, and there is a steady increase in thermal conductivity as nitrogen and oxygen in the surrounding air permeate into the cells to replace the CO_2 originally in the cells of the foam [12]. Such rise in gas thermal conductivity may take place for several months, and may have happened in the present foam specimen. However, the fraction of CO_2 remaining in the cells is difficult to estimate. Curve (e) in *figure 13* was considered for the limiting condition that all the CO_2 in the cells was replaced by air. In the present temperature range, the thermal conductivity of air is up to about 60 % higher than that of CO_2. Although the gas pressure in a cell varies with temperature, the pressure effect does not need to be considered because the thermal conductivity of a gas is basically independent of pressure [14, chapter 2].

Comparison of the five prediction curves in *figure 13* shows that the change in the value of k_p (curve (c)) increases the predicted k_{eff} for about 22 %, while assuming total air permeation into the cells (curve (e)) increases the predicted k_{eff} for about 19 %. Both decreasing ρ_s (curve (b)) and increasing f_s (curve (d)) increase the predicted k_{eff} for only about 6 %. Comparison between all the five predicted curves and both sets of experimental data suggests that the model by Glicksman et al. [5] underpredicts the k_{eff} of the present polyurethane foam specimen. The predicted curves based on the model are closer to the experimental data of Taylor et al. [11], while the present experimental data demonstrate greater slopes (dk_{eff}/dT) than the predicted curves. The large slopes of the present data may be due to the error caused by contraction of material during heating. More contraction of the foam material was observed at a higher temperature. There was a larger contraction in the central region on the heated surface than in the periphery. Therefore, the foam specimen surface in contact with the electric heater formed a shape of basin. As a result, in the central region of the heated surface, the thermal contact between the heater and the specimen deteriorated with temperature. The higher thermal resistance in the central region

redistributed heat flux, and the heat flux actually passing through that region was lower than the average value. The thermocouples located along the centerline of the specimen were directly influenced by this lower-than-average heat flux. This phenomenon caused an error in the measured effective thermal conductivity, and such an error increased with temperature. However, the maldistribution of heat flux due to bad thermal contact in the central region is difficult to quantify. As shown in the following error analysis, when a variation of $\pm 10\,\%$ in the heat flux is applied, both the resultant k_{eff} and C vary about $\pm 10\,\%$.

5. CONCLUSIONS

Thermal conductivity and heat capacity of polyurethane foam material were measured at elevated temperatures. Polyurethane foam specimens of 374 $\text{kg}\cdot\text{m}^{-3}$ density were tested up to 200 °C. Effective thermal conductivity and heat capacity were determined by parameter estimation analysis using transient temperature data taken across the foam specimen when one surface was heated by an electric heater. All data obtained were analyzed in terms of sequential estimates, residuals, sensitivity coefficients to assure accuracy. The effects of heater thermal conductivity and contact resistance between the heater and the specimen were found to be important. The present experimental result was higher than that predicted by an existing model.

Acknowledgement

This work was supported by Sandia National Laboratories under Project AV-7569.

REFERENCES

[1] Skochdopole R.E., The thermal conductivity of foam plastics, Engineering Progress 57 (0) (1961).

[2] Booth L.D., Radiation contribution as an element of thermal conductivity, in: Polyurethanes World Congress, 1987, pp. 85–90.

[3] Valenzuela J.A., Glicksman L.R., Thermal resistance and aging of rigid urethane foam insulation, in: DOE-ORNL Workshop on Mathematical Modeling of Roofs, Atlanta, CONF-811179, 1981, pp. 261–262.

[4] Cunnigham A., Jeffs G.M.F., Rosbotham I.D., Sparrow D.J., Recent advances in the development of rigid polyurethane foams of improved thermal insulation efficiency, in: Polyurethanes World Congress, 1987, pp. 104–110.

[5] Glicksman L.R., Marge A.L., Moreno J.D., Radiation heat transfer in cellular foam insulation, in: Developments in Radiation Heat Transfer, HTD Vol. 203, ASME, 1992, pp. 45–54.

[6] Schuetz M.A., Glicksman L.R., A basic study of heat transfer through foam insulation, Journal of Cellular Plastics (1984) 114–121.

[7] Khanpara J.C., Sirdeshpande G., Experimental evaluation of the effect of cell shape on heat and mass transfer through elastomeric foams, Journal of Thermal Insulation 13 (1990) 191–204.

[8] Beck J.V., Arnold K.J., Parameter Estimation in Engineering and Science, Wiley, 1977.

[9] Dowding K., Beck J., Ulbrich A., Blackwell B., Hayes J., Estimation of thermal properties and surface heat flux in carbon–carbon composite, Journal of Thermophysics and Heat Transfer 9 (1995) 345–351.

[10] Moffat R.J., Describing the uncertainties in experimental results, Experimental Thermal and Fluid Science 1 (1988) 3–17.

[11] Taylor R.E., Groot H., Ferrier J., Thermophysical properties of a foam and a pyromark paint 2500, TPRL 1833 Report to Sandia National Laboratories, April 1997.

[12] Collishaw P.G., Evans J.R.G., Review—an assessment of expression for the apparent thermal conductivity of cellular materials, Journal of Materials Science 29 (1994) 2261–2273.

[13] Dostal C.A. (Ed.), Engineering Materials Handbook, Vol. 2, American Society for Metals, 1988, p. 260.

[14] Incropera F.P., DeWitt D.P., Fundamentals of Heat and Mass Transfer, 4th edition, Wiley, 1996.

APPENDIX

Error analysis

The errors of the thermal property results obtained can be assessed by the method of sequential perturbations [10]. In this method, the total uncertainty of a set of data is estimated by integrating the uncertainties due to errors associated with individual parameters. In the present experiment, three major sources of error are

(a) the error in temperature data measured by thermocouples along with the data acquisition system,

(b) the error in the location of a thermocouple well caused by drifting during drilling a long, narrow hole, and

(c) the error in the input heat flux level due to material contraction and bad thermal contact, as discussed above.

The property data (k_{eff} and C) were first calculated by inverse conduction analysis using the measured temperature (T) data at given locations (x) and times, as well as assumed uniform input heat flux (q''). The uncertainty associated with the present temperature data, u_T, was then applied to all temperature data, and the inverse conduction analysis was conducted again. As a result of introduction of temperature uncertainty, the estimated property result, k_{eff}, varied by $\Delta(k_{\text{eff}})_T$. The variation in k_{eff} due to the uncertainty in x, $\Delta(k_{\text{eff}})_x$, as well

TABLE V
Values of parameters involved in error analysis.

Variable	Uncertainty	Resultant deviation	
T	$u_T = \pm 0.5$ K	$\Delta(k_{\text{eff}})_T / k_{\text{eff}} = 8\,\%$	$\Delta(C)_T / C = 4\,\%$
x	$u_x = \pm 0.05$ mm	$\Delta(k_{\text{eff}})_x / k_{\text{eff}} = 1\,\%$	$\Delta(C)_x / C = 1\,\%$
q''	$U_{q''} = \pm 10\,\%$	$\Delta(k_{\text{eff}})_{q''} / k_{\text{eff}} = 10\,\%$	$\Delta(C)_{q''} / C = 10\,\%$

TABLE VI
Temperature uncertainty values applied in trial cases to determine $\Delta(k_{\text{eff}})_T$ and $\Delta(C)_T$, data in K.

Case	Thermocouple location x, in					
	0.0	0.25	0.5	0.75	1.0	1.5
1	+0.5	+0.5	+0.5	+0.5	+0.5	+0.5
2	−0.5	−0.5	−0.5	−0.5	−0.5	−0.5
3	+0.5	+0.3	+0.1	−0.1	−0.3	−0.5
4	−0.5	−0.3	−0.1	+0.1	+0.3	+0.5
5	+0.5	−0.5	+0.5	−0.5	+0.5	−0.5
6	−0.5	+0.5	−0.5	+0.5	−0.5	+0.5

as that due to the uncertainty in q'', $\Delta(k_{\text{eff}})_{q''}$, were also estimated following the same method. Finally, the total uncertainty associated with k_{eff} was determined by

$$U_{k_{\text{eff}}} = \sqrt{\sum_i^3 \left[\frac{\Delta(k_{\text{eff}})_i}{k_{\text{eff}}} \right]^2} \tag{A.1}$$

where $\Delta(k_{\text{eff}})_i$ includes $\Delta(k_{\text{eff}})_T$, $\Delta(k_{\text{eff}})_x$, and $\Delta(k_{\text{eff}})_{q''}$. The uncertainty with C data was estimated following a similar method:

$$U_C = \sqrt{\sum_i^3 \left[\frac{\Delta(C)_i}{C} \right]^2} \tag{A.2}$$

The uncertainty values and the resultant deviations for individual variables in the present error analysis are listed in *table V*. The uncertainty with thermocouple location, u_x, was estimated to be very small since very little drifting would occur during drilling in a soft material such as foam. After drilling, the drill experienced no resistance moving in and out the hole, indicating a very straight hole. The uncertainty u_x was estimated as ± 0.05 mm.

TABLE VII
Thermocouple location uncertainty values applied in trial cases to determine $\Delta(k_{\text{eff}})_x$ and $\Delta(C)_x$, data in mm.

Case	Thermocouple location x, in					
	0.0	0.25	0.5	0.75	1.0	1.5
1	0.0	+0.05	+0.05	+0.05	+0.05	+0.05
2	0.0	−0.05	−0.05	−0.05	−0.05	−0.05
3	0.0	+0.05	−0.05	+0.05	−0.05	+0.05
4	0.0	−0.05	+0.05	−0.05	+0.05	−0.05

The deviation in k_{eff} due to temperature, $\Delta(k_{\text{eff}})_T$, was determined as the maximum possible deviation in k_{eff} as a result of a maximum ± 0.5 K uncertainty applied to all temperature data. The cases considered were exhibited in *table VI*. The maximum $\Delta(k_{\text{eff}})_T$ and $\Delta(C)_T$ were given by case 6 featuring an alternate $\pm$ uncertainty pattern.

The deviation in k_{eff} due to thermocouple location, $\Delta(k_{\text{eff}})_x$, was determined as the maximum possible deviation in k_{eff} as a result of a maximum ± 0.05 mm uncertainty applied to all thermocouple location data. The cases considered were exhibited in *table VII*. The maximum $\Delta(k_{\text{eff}})_x$ and $\Delta(C)_x$ were given by case 3 or 4, depending on temperature. Finally, using equations (8) and (9), the total uncertainty in k_{eff} is calculated as $\pm 13\,\%$, and the total uncertainty in C is $\pm 11\,\%$.